

# Spectral Analysis of Relativistic Bunched Beams

R. H. Siemann\*

*Stanford Linear Accelerator Center, Stanford University, Stanford, CA 94309*

## INTRODUCTION

Particles in a storage ring are oscillating in the longitudinal and transverse dimensions, and therefore, the frequency domain is natural for analyzing many beam generated signals. Information ranging from oscillation frequencies to beam phase space distributions can be extracted from the spectral content of these signals.

It is often necessary to switch between time and frequency domains using Fourier transforms. If  $f(t)$  is a function of time,  $F(\omega)$  given by

$$F(\omega) = \int_{-\infty}^{\infty} f(t)e^{-j\omega t} dt \quad (1)$$

is its Fourier transform. In this equation  $j = \sqrt{-1}$  and  $\omega$  is the angular frequency which is the appropriate mathematical variable rather than the frequency  $\nu = \omega/2\pi$  that is measured by spectrum analyzers. The meaning of the word "frequency" depends on context, but the notation  $\nu$  for frequency and  $\omega$  for angular frequency will be rigorous. The inverse transform is

$$f(t) = \frac{1}{2\pi} \int_{-\infty}^{\infty} F(\omega)e^{j\omega t} d\omega . \quad (2)$$

These notes are restricted to relativistic beams, and for these beams the image current flowing in the walls of an accelerator vacuum chamber,  $i_w$ , has a line density equal to the line density of the beam current,  $i_b$ ,

$$i_w(t) = -i_b(t) \text{ and } I_w(\omega) = -I_b(\omega) \quad (3)$$

with an overall minus sign since it is an image current. The image current is an ideal current source; nothing placed in the vacuum chamber wall can affect it

---

\* Work supported by the Department of Energy, contract DE-AC03-76SF00515.

because the beam would have to be decelerated for that to happen. The image current flowing through a beam detector produces a voltage  $V_{\text{out}}$  given by

$$V_{\text{out}}(\omega) = I_w(\omega)S(\omega) \quad (4)$$

where  $S$  is the detector longitudinal sensitivity. The sensitivity depends on the detector, on whether it is a cavity, strip line, capacitive pickup, etc., and  $S(\omega)$  can vary rapidly or slowly with frequency. I am assuming the variation is slow, and that the spectrum of the output voltage is the same as that of the wall and beam currents. Many measurements can be made in a narrow frequency band where the sensitivity can be treated as a constant, so this is a good approximation. If it isn't, corrections must be made to account for frequency dependence of the sensitivity.

If the beam is offset from the vacuum chamber center, the image current is not uniform; instead, it varies around the beam pipe due to the displacement of the beam. A transverse beam detector responds to the dipole moment

$$d(t) = i_b(t)r_{\perp}(t) \quad (5)$$

where  $r_{\perp}(t)$  is the displacement from the center. The output voltage of a transverse detector is

$$V_{\text{out}}(\omega) = D(\omega)S_{\Delta}(\omega) \quad (6)$$

where  $S_{\Delta}$  and  $D$  are the transverse sensitivity and the Fourier transform of the dipole moment, respectively. As with the longitudinal,  $S_{\Delta}$  is assumed to vary slowly with frequency, and corrections must be made if that isn't a good approximation.

## A SINGLE PARTICLE

The spectrum of a single particle is like a Green's function, and it is the key to understanding the spectrum produced by a beam. Three separate cases are considered in an order of increasing complexity: 1) constant revolution frequency, 2) Frequency Modulation introduced by synchrotron oscillations, and 3) Amplitude Modulation introduced by betatron oscillations.

### Longitudinal Motion & Constant Revolution Frequency

The current of a single, unit-charge particle with a constant revolution frequency  $\omega_r$ , Figure 1, is a periodic set of impulses spaced a time  $T = 2\pi/\omega_r$  apart

$$i_b(t) = \sum_{n=-\infty}^{\infty} \delta(t - nT). \quad (7)$$

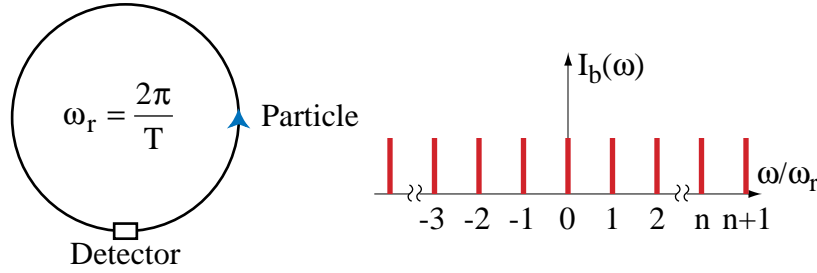


**Figure 1.** A particle with a constant revolution frequency passing a beam detector located at one point in the ring and the spectrum it produces.

Fourier transforming this gives

$$\begin{aligned}
 I_b(\omega) &= \int_{-\infty}^{\infty} i_b(t) e^{-j\omega t} dt = \int_{-\infty}^{\infty} \sum_{n=-\infty}^{\infty} \delta(t - nT) e^{-j\omega t} dt \\
 &= \sum_{n=-\infty}^{\infty} e^{-j\omega nT} = \sum_{n=-\infty}^{\infty} e^{-j2\pi n \omega / \omega_r} .
 \end{aligned} \tag{8}$$

The last sum is an infinite sum of unit magnitude phasors. If these phasors are at different angles they will add up to zero because there is an infinite number of them, but if they are all at the same angle the sum will be infinite. The latter happens when  $\omega/\omega_r$  equals an integer; every angle is an integer multiple of  $2\pi$  in that case. This is written formally as

$$I_b(\omega) = \sum_{n=-\infty}^{\infty} e^{-j2\pi n \omega / \omega_r} = \omega_r \sum_{n=-\infty}^{\infty} \delta(\omega - n\omega_r). \tag{9}$$

The spectrum is a comb of equal amplitude lines spaced at  $\omega_r$  extending from  $\omega = -\infty$  to  $\omega = \infty$ . It is shown in Figure 1. The spectrum has two properties - the **frequencies** that are given by the argument of the  $\delta$ -function and the **envelope** that is given by the factor in front. The frequencies are harmonics of  $\omega_r$ , and the envelope equals  $\omega_r$  independent of frequency.

There are both positive and negative frequencies in eq. 9, but spectrum analyzers measure only positive frequencies. How should the negative frequencies be interpreted? Fourier transforming to the time domain

$$i_b(t) = \frac{\omega_r}{2\pi} \sum_{n=-\infty}^{\infty} e^{jn\omega_r t} . \tag{10}$$

Each term in the sum is unit magnitude phasor. The angles of the positive frequency phasors increase with time while those of the negative phasors decrease with time. The phasors for the same  $|n|$  are shown in Figure 2. The real parts are in phase, and the imaginary parts are 180° out of phase. The physically meaningful quantity is the real part that is given by

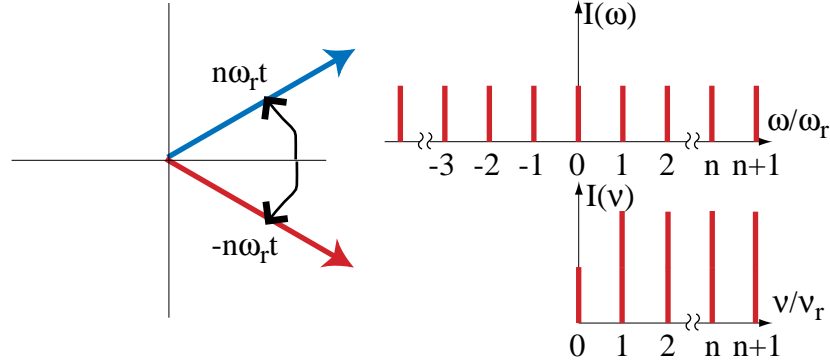


**Figure 2.** Positive and negative frequency phasors for the same  $|n|$  and the mathematical and measured, physical spectra. The line at  $n = 0$  is one-half that for  $n \neq 0$  because there is no corresponding negative frequency line .

$$\Re(e^{jn\omega_r t} + e^{-jn\omega_r t}) = 2 \cos(n\omega_r t) \quad (11)$$

The positive and negative frequency phasors appear in phase and at the same at the same frequency on the spectrum analyzer. The resulting spectrum is shown in Figure 2.

## Frequency Modulation Introduced By Synchrotron Oscillations

Synchrotron motion modulates the arrival time by

$$\tau = \tau_a \cos(\omega_s t + \varphi) \quad (12)$$

where  $\tau_a$  is the synchrotron oscillation amplitude,  $\omega_s$  is the synchrotron frequency and  $\varphi$  is the phase.\* Instead of being a series of impulses spaced exactly  $T$  apart, the current is

$$i_b(t) = \sum_{n=-\infty}^{\infty} \delta(t - [nT + \tau_a \cos(\omega_s nT + \varphi)]) . \quad (13)$$

where  $\tau_a$  is the synchrotron oscillation amplitude,  $\omega_s$  is the synchrotron frequency and  $\varphi$  is the phase at  $n = 0$ . The synchrotron frequency and synchrotron tune  $Q_s$  are related by  $\omega_s = Q_s \omega_r$ . The Fourier transform is

\* The synchrotron frequency and synchrotron tune  $Q_s$  are related by  $\omega_s = Q_s \omega_r$ .

$$I_b(\omega) = \sum_{n=-\infty}^{\infty} \exp(-j\omega[nT + \tau_a \cos(\omega_s nT + \varphi)]) . \quad (14)$$

In the limit of small amplitude or low frequency,  $\omega\tau_a \ll 1$ , the second term in the exponent can be approximated with a Taylor expansion

$$\begin{aligned} I_b(\omega) &\approx \sum_{n=-\infty}^{\infty} e^{-jn\omega T} (1 - j\omega\tau_a \cos(\omega_s nT + \varphi)) \\ &= \sum_{n=-\infty}^{\infty} e^{-jn\omega T} \left( 1 - \frac{j\omega\tau_a}{2} e^{j(\omega_s nT + \varphi)} - \frac{j\omega\tau_a}{2} e^{-j(\omega_s nT + \varphi)} \right) . \end{aligned} \quad (15)$$

The first of the three sums is the same as for a constant revolution frequency. Take a look at the second one;

$$\begin{aligned} \sum_{n=-\infty}^{\infty} \exp(-jn\omega T + j\omega_s nT + j\varphi) &= e^{j\varphi} \sum_{n=-\infty}^{\infty} \exp(-j2\pi n(\omega - \omega_s)/\omega_r) \\ &= e^{j\varphi} \sum_{n=-\infty}^{\infty} \delta(\omega - \omega_s - n\omega_r) . \end{aligned} \quad (16)$$

The last step follows from the same logic used for a constant revolution frequency - the sum equals zero unless  $(\omega - \omega_s)/\omega_r$  is an integer. The frequencies differ from the rotation harmonics by  $+\omega_s$ . The third term in eq. 15 leads to frequencies that differ from the rotation harmonics by  $-\omega_s$ . Synchrotron motion has lead to two new frequency combs displaced from the rotation harmonics. Both of these combs have envelopes that depend linearly on frequency.

The approximation in eq. 15 is valid for small amplitudes and/or low frequencies. The Taylor series expansion could be continued. The next term would affect the envelope of the rotation harmonics and introduce frequency combs displaced from the rotation harmonics by  $\pm 2\omega_s$ . However, rather than doing this it is better to perform a Bessel function expansion<sup>1</sup>

$$e^{-jz \cos \theta} = \sum_{k=-\infty}^{\infty} J_k(z) e^{jk(\theta - \pi/2)} \quad (17)$$

where  $J_k$  is an ordinary Bessel function of order  $k$ . This same expansion leads to Bessel functions in every analysis of Frequency Modulation. Using this in eq. 14

$$\begin{aligned} I_b(\omega) &= \sum_{n,k=-\infty}^{\infty} J_k(\omega\tau_a) e^{jk(\omega_s nT + \varphi - \pi/2)} e^{-jn\omega T} \\ &= \sum_{n,k=-\infty}^{\infty} e^{jk(\varphi - \pi/2)} J_k(\omega\tau_a) e^{-j2\pi n(\omega - k\omega_s)/\omega_r} . \end{aligned} \quad (18)$$

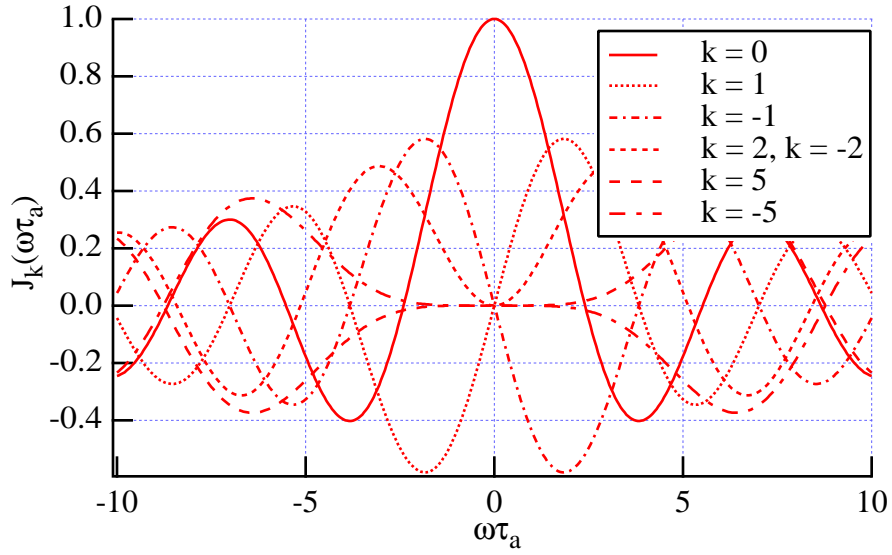


**Figure 3.** The envelopes for different synchrotron sidebands and  $\varphi = \pi/2$ .

As before the summation over  $n$  restricts the possible frequencies. In this case it requires that  $(\omega - k\omega_s)/\omega_r$  equals an integer. Performing the sum

$$I_b(\omega) = \omega_r \sum_{k=-\infty}^{\infty} e^{jk(\varphi-\pi/2)} J_k(\omega\tau_a) \sum_{n=-\infty}^{\infty} \delta(\omega - k\omega_s - n\omega_r). \quad (19)$$

Equation 19 gives the general expression for the spectrum of a particle undergoing synchrotron motion. It is an important result that deserves substantial discussion.

1. The approximate treatment based on a Taylor expansion corresponds to three of the terms,  $k = -1, 0, 1$ , when the lowest order Taylor expansions for the Bessel functions are used.
2. For each rotation harmonic there is an infinite number of sidebands. They are displaced from the rotation harmonic by  $k\omega_s$ ,  $k = -\infty, \dots, \infty$  and have different envelopes. The envelopes illustrated in Figure 3 have the usual properties of ordinary Bessel functions: *i*) they are even (odd) functions of  $\omega\tau_a$  if  $k$  is even (odd) and *ii*) the first maximum of  $J_k$  is at  $\omega\tau_a \approx k$ . When  $|\omega| \ll 1/\tau_a$  only the rotation harmonics,  $k=0$ , are present, and as the frequency increases more sidebands appear. This is illustrated in Figure 4.
3. The synchrotron sideband number,  $k$ , appears in two different places: *i*) the frequency shift from the rotation harmonic is  $k\omega_s$ , and *ii*) the envelope is  $J_k(\omega\tau_a)$ . The best frequency region to observe the  $k$ th sideband is at  $\omega \sim k/\tau_a$ . This connection between frequency shift and frequency region for observation will become important when the phase space structure of a beam is considered.

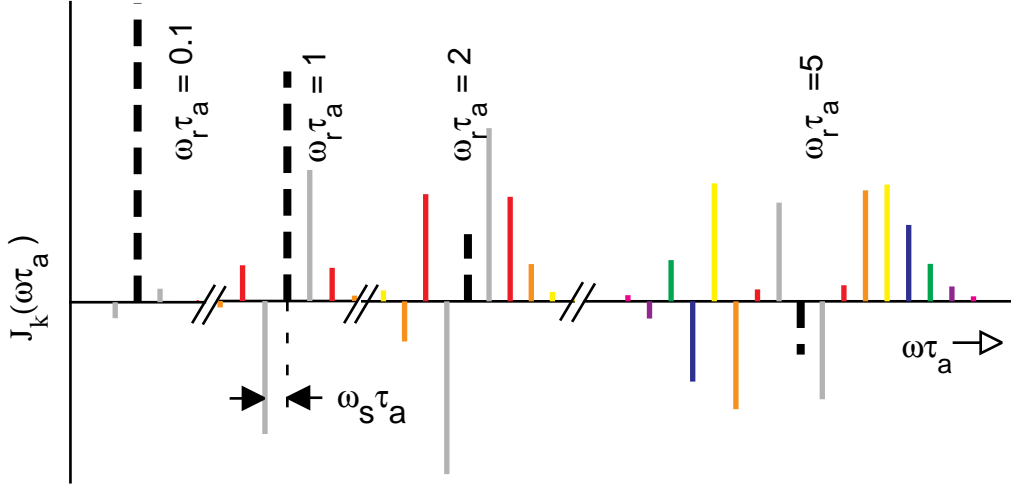


**Figure 4.** The spectra for different  $\omega_r\tau_a$  for a synchrotron tune  $Q_S = 0.01$  and  $\phi = \pi/2$ . The heavy dashed line is  $k = 0$  in each case

4. The phase  $\phi$  is the phase of the synchrotron oscillation when  $n = 0$ . Since the sum is infinite,  $n = 0$  is arbitrary, and, therefore,  $\phi$  is arbitrary. This situation changes when multiple particles are considered, and the phases of the particles relative to each other has significance.
5. The observed spectrum is obtained by combining the positive and negative frequency components. The signals at  $\omega = \omega_{nk} = n\omega_r + k\omega_s$  and  $\omega = -\omega_{nk}$  have the same physical frequency, and as the next line shows, they add coherently in the physical spectrum. Fourier transforming back to the time domain and taking the real part gives

$$\begin{aligned}
& \Re(i_b(t)) \\
&= \Re\left[e^{jk(\phi-\pi/2)}J_k(\omega_{nk}\tau_a)e^{j\omega_{nk}t} + e^{-jk(\phi-\pi/2)}J_{-k}(-\omega_{nk}\tau_a)e^{-j\omega_{nk}t}\right] \quad (20) \\
&= 2J_k(\omega_{nk}\tau_a)\cos(\omega_{nk}t + k\phi - k\pi/2) .
\end{aligned}$$

## Amplitude Modulation Introduced By Betatron Oscillations

### *Constant Revolution Frequency*

A particle can be offset from the center of a transverse beam detector due to closed orbit errors, synchrotron oscillations combined with dispersion, or betatron oscillations. A closed orbit offset produces a spectrum identical to that

of longitudinal motion alone. Synchrotron oscillations combined with dispersion do not introduce new frequencies although they do affect the envelopes.<sup>2</sup> Betatron motion produces Amplitude Modulation that leads to new frequencies and new phenomena in the spectrum. The next two sections concentrate on betatron motion.

Begin with a constant revolution frequency. The displacement is given by

$$r_{\perp}(t) = A_{\beta} \cos \omega_{\beta} t = \frac{A_{\beta}}{2} (e^{j\omega_{\beta} t} + e^{-j\omega_{\beta} t}) \quad (21)$$

where  $A_{\beta}$  is the betatron amplitude, and  $\omega_{\beta}$  is the betatron frequency that is related to the betatron tune,  $Q_{\beta 0}$ , by  $Q_{\beta 0} = \omega_{\beta} / \omega_r$ . The dipole moment and its Fourier transform are

$$d(t) = i_b(t) r_{\perp}(t) = \frac{A_{\beta}}{2} (e^{j\omega_{\beta} t} + e^{-j\omega_{\beta} t}) \sum_{n=-\infty}^{\infty} \delta(t - nT), \quad (22)$$

and

$$\begin{aligned} D(\omega) &= \frac{A_{\beta}}{2} \left[ \sum_{n=-\infty}^{\infty} e^{-j(\omega - \omega_{\beta})nT} + \sum_{n=-\infty}^{\infty} e^{-j(\omega + \omega_{\beta})nT} \right] \\ &= \frac{A_{\beta} \omega_r}{2} \left[ \sum_{n=-\infty}^{\infty} \delta(\omega - \omega_{\beta} - n\omega_r) + \sum_{n=-\infty}^{\infty} \delta(\omega + \omega_{\beta} - n\omega_r) \right]. \end{aligned} \quad (23)$$

There are two frequency combs. One is displaced from the rotation harmonics by  $+\omega_{\beta}$  and the other by  $-\omega_{\beta}$ . Each has a constant envelope. This is illustrated in Figure 5. The betatron tune is almost always greater than one, and, as consequence of measuring the dipole moment at only one point on the orbit, the integer part of the tune cannot be measured from the spectrum.

There is also an ambiguity in measuring the fractional part of the tune. The spectrum when the fractional part of the tune equals  $q_{\beta}$  is the same as when the fractional part equals  $1 - q_{\beta}$ . Figures 5b and 5d illustrate this. The ambiguity arises because AM produces sidebands above and below the rotation harmonics. One way to resolve it is to increase the tune by strengthening a focusing quadrupole and observing whether the spectral line moves to lower or higher frequency. The frequency of a line in the region  $n\omega_r < \omega < (n + 1/2)\omega_r$  will increase if  $q_{\beta} < 0.5$ , and it will decrease if  $q_{\beta} > 0.5$ .

The physical spectra in Figures 5b, 5d could have been derived in a different way. Rather than using eq. 21 for the transverse displacement,  $r_{\perp}$  could have been written

$$r_{\perp}(t) = A_{\beta} e^{j\omega_{\beta} t}. \quad (24)$$

This would have resulted in a mathematical spectrum with only upper sidebands of amplitude  $A_{\beta}$ . However, when the real part of the resulting expression was



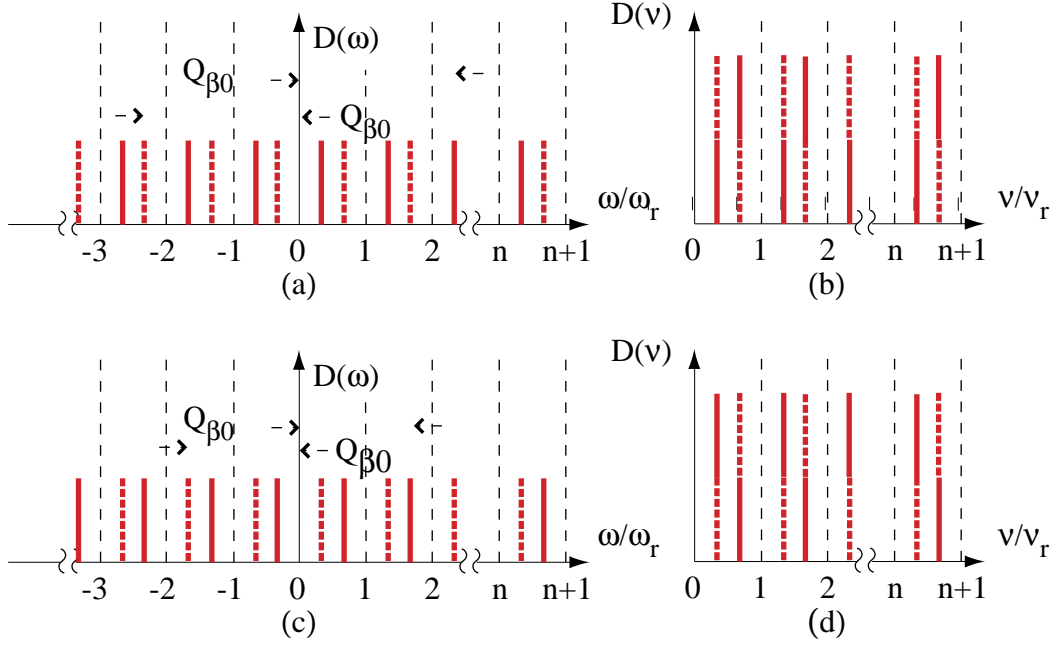


**Figure 5.** The mathematical (a, c) and physical (b, d) spectra given by eq. 23 when  $Q_{\beta 0} \approx 2.33$  (a, b) and  $Q_{\beta 0} \approx 1.66$  (c, d). For purposes of illustration the lines from one comb are solid and the lines from the other comb are dashed.

taken, the physical spectra would be the same as in Figures 5b and 5d. A generalization of eq. 24 is the more convenient form for the transverse displacement when the effects of synchrotron oscillations are included.

### *Betatron and Synchrotron Motion*

The focusing strength of a quadrupole depends on energy, and energy is modulated by synchrotron motion. As a result, the betatron phase does not advance smoothly. The generalization of eq. 24 in terms of the betatron phase  $\psi_{\beta}$  is

$$r_{\perp}(t) = A_{\beta} e^{j\psi_{\beta}(t)} . \quad (25)$$

The time rate of change of  $\psi_{\beta}$  is

$$\frac{d\psi_{\beta}}{dt} = \omega_{\beta}(1 + \xi\delta) + O(\delta^2) \quad (26)$$

where  $\delta$  is the fractional deviation from the central energy and  $\omega_{\beta} = Q_{\beta 0}\omega_r$  is the betatron frequency when  $\delta = 0$ . The chromaticity,  $\xi$ , measures the variation of betatron tune with energy. It is defined as

$$\xi = \frac{1}{Q_{\beta 0}} \left. \frac{dQ_{\beta}(\delta)}{d\delta} \right|_{\delta=0} . \quad (27)$$

The energy deviation is 90° out of phase with the time deviation,  $\tau$

$$\delta = \frac{1}{\alpha} \frac{d\tau}{dt} = -\frac{\omega_s \tau_a}{\alpha} \sin(\omega_s t + \varphi) \quad (28)$$

where  $\alpha$  is the momentum compaction. Substituting this into eq. 26 and integrating gives

$$\psi_{\beta}(t) = \omega_{\beta} t + \omega_{\xi} \tau_a \cos(\omega_s t + \varphi) + \psi . \quad (29)$$

The chromatic frequency is  $\omega_{\xi} = \omega_{\beta} \xi / \alpha$ , and  $\psi$  is a constant of integration related to the betatron phase at  $t = 0$  by

$$\psi = \psi_{\beta}(t=0) - \omega_{\xi} \tau_a \cos \varphi = \psi_{\beta}(t=0) - \omega_{\xi} \tau(t=0) . \quad (30)$$

The dipole moment is

$$d(t) = i_b(t) r_{\perp}(t) = A_{\beta} e^{j\psi_{\beta}(t)} \sum_{n=-\infty}^{\infty} \delta(t - [nT + \tau_a \cos(\omega_s nT + \varphi)]) . \quad (31)$$

Following the procedure developed above, and identifying the important frequencies gives

$$\begin{aligned} D(\omega) &= \omega_r A_{\beta} e^{j\psi} \sum_{k=-\infty}^{\infty} e^{jk(\varphi - \pi/2)} J_k((\omega - \omega_{\beta} - \omega_{\xi})\tau_a) \\ &\times \sum_{n=-\infty}^{\infty} \delta(\omega - (n\omega_r + k\omega_s + \omega_{\beta})) . \end{aligned} \quad (32)$$

This result gives the general expression for the transverse spectrum of a particle undergoing betatron and synchrotron oscillations and is comparable in importance to eq. 19 .

1. There are an infinite number of synchrotron sidebands centered about the betatron frequencies. These sidebands are displaced from the betatron lines by  $k\omega_s$ ,  $k = -\infty, \dots, \infty$ .
2. The envelopes are ordinary Bessel functions with argument  $(\omega - \omega_{\beta} - \omega_{\xi})\tau_a$ . In contrast to the longitudinal, these envelopes are offset from  $\omega = 0$  by  $\omega_{\beta} - \omega_{\xi} \approx \omega_{\xi}$  since typically  $\omega_{\beta} \ll \omega_{\xi}$ . A positive chromaticity shifts the envelopes to positive frequencies, etc. This is illustrated in Figure 6.
3. The envelope of sideband  $k$  is  $J_k((\omega - \omega_{\xi})\tau_a)$ . The best frequency region to observe the  $k$ th sideband is at  $\omega \sim \omega_{\xi} + k/\tau_a$ . Depending on the chromatic frequency, high order sidebands can be seen at low frequencies.
4. The phase of the betatron oscillation when  $n = 0$  only has meaning for multiple particles.

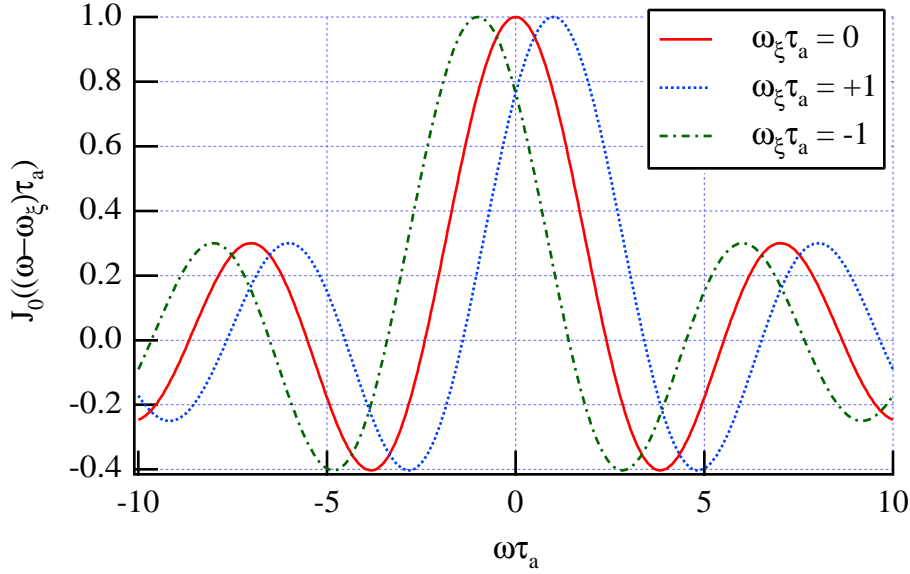


**Figure 6.** Envelopes for the betatron line ( $k = 0$ ) for three different values of chromatic frequency.

5. The observed spectrum is obtained by combining the positive and negative frequencies as has been done above. The mathematical spectrum based on eq. 25 has only upper sidebands, but the physical spectrum has both upper and lower sidebands. The lower sidebands come from negative frequencies in this mathematics.

## MULTIPLE PARTICLES

The expressions in eqs. 19 and 32 are the basis for understanding beam generated signals. For example, the longitudinal spectrum of a beam can be derived by convoluting eq. 19 with the longitudinal phase space density of the beam,  $\rho(\tau_a, \phi)$ , where  $\rho\tau_a d\tau_a d\phi$  is the charge in phase space area  $\tau_a d\tau_a d\phi$ ;

$$\mathbf{I}(\omega) = \omega_r \sum_{k,n=-\infty}^{\infty} \delta(\omega - k\omega_s - n\omega_r) \int_0^{\infty} \tau_a d\tau_a \int_0^{2\pi} d\phi \rho(\tau_a, \phi) e^{jk\phi} J_k(\omega\tau_a). \quad (33)$$

The envelope has changed, but the frequencies haven't.

The examples below will show how information about the beam can be extracted from spectra. These examples are intended to illustrate methods that can be applied to many problems.

## Longitudinal Phase Space Structure

When beam intensity is low, particle motion is determined by magnet and RF cavity fields. Beam generated fields can be neglected, and particles move independently of each other. The longitudinal phase space density can depend on  $\tau_a$ , but it can't depend on  $\phi$ . If it did, particles would not be independent.\* The phase space density is  $\rho(\tau_a, \phi) = \rho_0(\tau_a)/2\pi$ , and the beam generated signal is

$$\begin{aligned} \mathbf{I}(\omega) &= \omega_r \sum_{k, n=-\infty}^{\infty} \delta(\omega - k\omega_s - n\omega_r) \int_0^{\infty} \tau_a d\tau_a \frac{1}{2\pi} \int_0^{2\pi} d\phi \rho_0(\tau_a) e^{jk\phi} J_k(\omega\tau_a) \\ &= \omega_r \sum_{n=-\infty}^{\infty} \delta(\omega - n\omega_r) \int_0^{\infty} \tau_a d\tau_a \rho_0(\tau_a) J_0(\omega\tau_a) . \end{aligned} \quad (34)$$

Only the  $k = 0$  term is not equal to zero once the  $\phi$  integral is performed. There are rotation harmonics but no synchrotron sidebands.

If the beam has charge  $Q$  and is Gaussian in  $\tau$  with rms bunch length  $\sigma_\tau$ ,

$$\rho_0(\tau_a) = \frac{Q}{\sigma_\tau} \exp(-\tau_a^2/2\sigma_\tau^2) , \quad (35)$$

and<sup>3</sup>

$$\mathbf{I}(\omega) = Q\omega_r \exp(-\omega^2\sigma_\tau^2/2) \sum_{n=-\infty}^{\infty} \delta(\omega - n\omega_r) . \quad (36)$$

The spectrum is a comb of rotation harmonics with a Gaussian envelope with rms width of  $1/\sigma_\tau$ . A detector with a flat sensitivity up to  $\omega \sim 1/\sigma_\tau$  can be used to measure the bunch length. Alternatively, an amplitude measurement at a fixed frequency of  $\omega \sim 1/\sigma_\tau$  could be used to monitor changes in bunch length.

The appearance of synchrotron sidebands and azimuthal structure in longitudinal phase space are directly related. Observation of synchrotron sidebands implies azimuthal phase space structure, and azimuthal phase space structure leads to synchrotron sidebands. Phase space structure arises from interaction of the beam with its own fields. Since these fields depend on the bunch distribution, that distribution is the solution of a self consistency problem formulated using the Vlasov Equation.<sup>4</sup>

The phase space density can be written as a Fourier expansion

$$\rho(\tau_a, \phi) = \frac{1}{2\pi} \sum_{m=-\infty}^{\infty} \rho_m(\tau_a) e^{im\phi} . \quad (37)$$

Substituting into eq. 33

---

\* This holds down to the Schottky noise level of the beam.

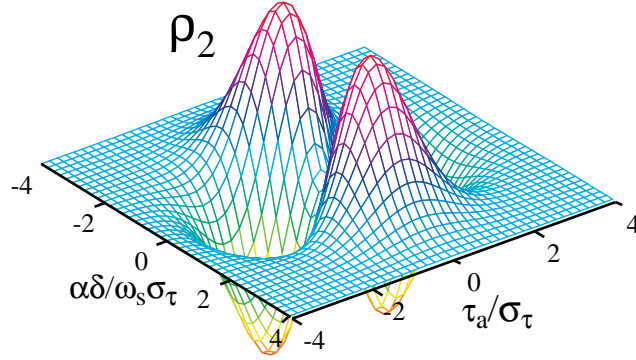


**Figure 7.** Phase space for the quadrupole perturbation given by eq. 39.

$$\begin{aligned}
\mathbf{I}(\omega) &= \frac{\omega_r}{2\pi} \sum_{k,n,m=-\infty}^{\infty} \delta(\omega - k\omega_s - n\omega_r) \int_0^{\infty} \tau_a d\tau_a \int_0^{2\pi} d\phi \rho_m(\tau_a) e^{j(k+m)\phi} J_k(\omega\tau_a) \\
&= \omega_r \sum_{m,n=-\infty}^{\infty} \delta(\omega + m\omega_s - n\omega_r) \int_0^{\infty} \tau_a d\tau_a \rho_m(\tau_a) J_k(\omega\tau_a).
\end{aligned} \tag{38}$$

There is a direct relation between each sideband and a specific harmonic of the phase space structure; the  $m$ th harmonic of the phase space structure produces a signal at the  $-k$ th sideband.

As a specific example, suppose that the beam has a quadrupole perturbation illustrated in Figure 7

$$\rho(\tau_a, \phi) = \frac{\rho_0(\tau_a)}{2\pi} \left( 1 + A_2 \frac{\tau_a^2}{\sigma_\tau^2} \cos(2\phi) \right) \tag{39}$$

where  $\rho_0$  is given by eq. 35. The  $\tau_a$  dependence of the perturbation was chosen for the purpose of this example. Substituting eq. 39 into 38 and performing the integrals<sup>3</sup>

$$\begin{aligned}
\mathbf{I}(\omega) &= Q\omega_r \exp(-\omega^2\sigma_\tau^2/2) \left[ \sum_{n=-\infty}^{\infty} \delta(\omega - n\omega_r) \right. \\
&\quad \left. + A_2 \frac{\omega^2\sigma_\tau^2}{2} \left( \sum_{n=-\infty}^{\infty} \delta(\omega - n\omega_r + 2\omega_s) + \sum_{n=-\infty}^{\infty} \delta(\omega - n\omega_r - 2\omega_s) \right) \right].
\end{aligned} \tag{40}$$

There are rotation harmonics and sidebands at  $\pm 2\omega_s$ . The envelopes are shown in Figure 8. The sideband signal is a maximum at  $\omega \sim 1.5/\sigma_\tau$  and is about a factor of 100 less than the rotation harmonics in this frequency range for  $A_2 = 0.01$ .

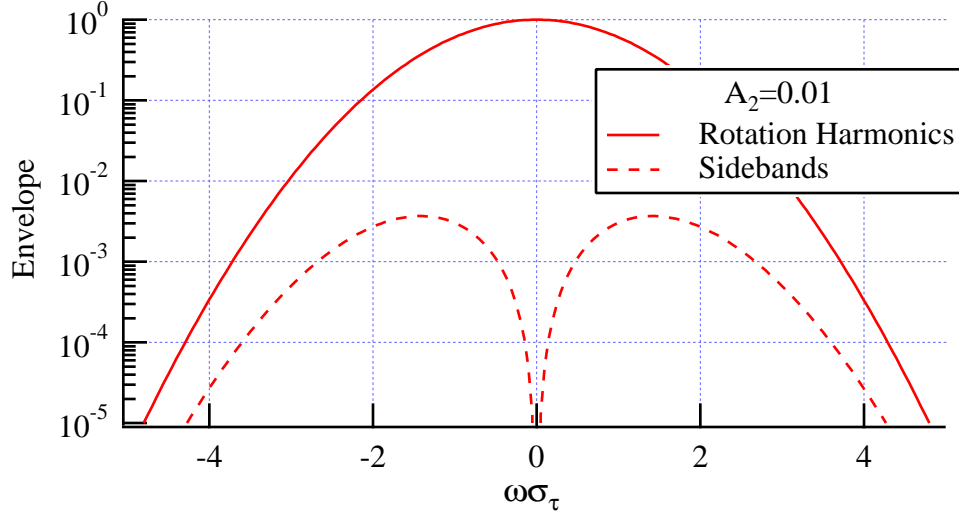


**Figure 8.** The envelopes for the rotation harmonics and second synchrotron sidebands for the example in eq. 39.

## Longitudinal Schottky Noise

Particles move independently of each other when beam generated fields are negligible, and it was argued in the previous section that a consequence is that the longitudinal phase space density,  $\rho(\tau_a, \varphi)$ , cannot depend on  $\varphi$ . However, there is a limit to this because a beam consists of individual particles not a smooth distribution. The particles cannot arrange themselves to remove all  $\varphi$  dependence. They wouldn't be independent if they could. There is some residual  $\varphi$  dependence and some signal, called Schottky noise, from it.

Taking account of individual particles, the phase space density is

$$\rho(\tau_a, \varphi) = q \sum_{p=1}^P \delta(\tau_a - \tau_{ap}) \delta(\varphi - \varphi_p) \quad (41)$$

where  $q$  is the particle charge,  $\tau_{ap}$  and  $\varphi_p$  are the amplitude and phase of the  $p$ th particle, and there are  $P$  particles in the beam. Using this distribution, eq. 33 becomes

$$\begin{aligned} \mathbf{I}(\omega) &= \sum_{k,n=-\infty}^{\infty} \delta(\omega - k\omega_s - n\omega_r) I_{nk}(\omega); \\ I_{nk}(\omega) &= q\omega_r \sum_{p=1}^P e^{jk\varphi_p} J_k(\omega_{nk} \tau_{ap}); \omega_{nk} = k\omega_s + n\omega_r. \end{aligned} \quad (42)$$

The current depends on the phase space coordinates of P particles, and it is different for every ensemble of particles.

This is just like a random walk problem. The result of a random walk is unknowable, but statistical quantities based on an ensemble of random walks have meaning. The relationship between the phase space coordinates of different particles changes with time due to non-linearities and random processes such as emission of synchrotron radiation photons. Therefore, while the current at a particular time is unknowable, the mean and rms currents are meaningful statistical quantities. They can be determined by averaging over all possible samples of P particles. This averaging is denoted by angular brackets,  $\langle \rangle$ 's.

Each of the terms in the expression for  $I_{nk}$  (eq. 42) is a phasor with magnitude given by the Bessel function and direction given by the argument of the exponential. When  $k \neq 0$ , the phasors point in all directions, and when averaged over all possible samples  $\langle I_{nk} \rangle = 0$ . The phase which had no meaning for a single particle is critically important for a beam. When  $k = 0$  all the phasors point in the same direction, and the sum does not vanish. The discrete particle nature of the beam is critical for evaluating the phasor sum, but once that is done the sum over particles can be evaluated with an integral using the phase space density  $\rho_0(\tau_a)$ . The mean current,  $\langle I_{n0} \rangle$ , is given eq. 34.

The square of the rms current is given by

$$\begin{aligned} \langle I_{nk}^2(\omega_{nk}) \rangle &= \frac{1}{2} \langle I_{nk}(\omega_{nk}) I_{nk}^*(\omega_{nk}) \rangle \\ &= \frac{q^2 \omega_r^2}{2} \left\langle \sum_{p=1}^P e^{jk\phi_p} J_k(\omega_{nk} \tau_{ap}) \sum_{s=1}^P e^{-jk\phi_s} J_k(\omega_{nk} \tau_{as}) \right\rangle \quad (43) \\ &= \frac{q^2 \omega_r^2}{2} \left\langle \sum_{p,s=1}^P e^{jk(\phi_p - \phi_s)} J_k(\omega_{nk} \tau_{ap}) J_k(\omega_{nk} \tau_{as}) \right\rangle . \end{aligned}$$

The terms in the double sum are phasors. In general they point in arbitrary directions making the sum equal to zero when the average is taken. However, for any sample of P particles the phasors line up and add coherently when  $\phi_p = \phi_s$ ; i.e. when particle p is the same as particle s. This removes one of the sums, and

$$\begin{aligned} \langle I_{nk}^2(\omega_{nk}) \rangle &= \frac{q^2 \omega_r^2}{2} \left\langle \sum_{p=1}^P J_k^2(\omega_{nk} \tau_{ap}) \right\rangle \\ &= \frac{q \omega_r^2}{2} \int_0^\infty \tau_a d\tau_a \rho_0(\tau_a) J_k^2(\omega_{nk} \tau_a) . \quad (44) \end{aligned}$$

The sum over particles has been replaced by an integral over  $\tau_a$  in the last step. When the beam is Gaussian and  $\rho_0$  is given by eq. 35<sup>5</sup>

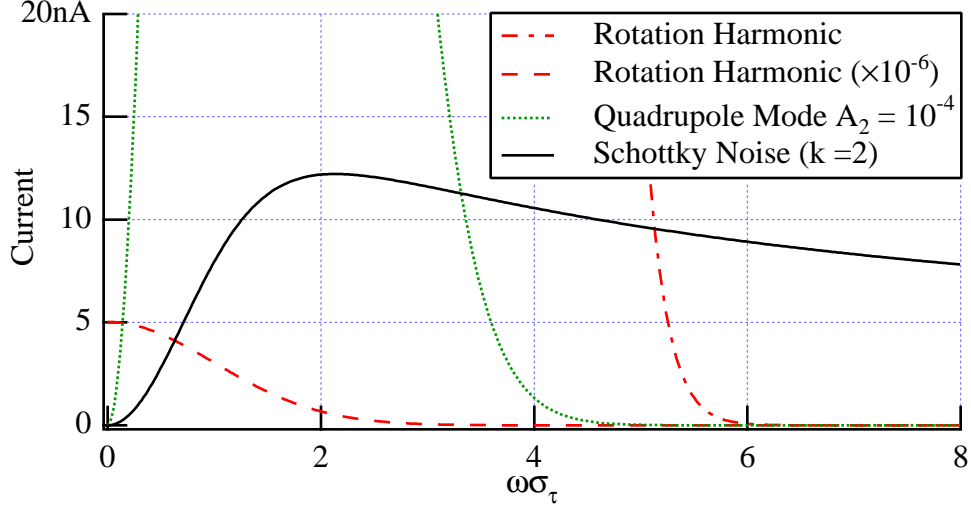


**Figure 9.** Envelopes for the rotation harmonics, a coherent structure with  $A_2 = 10^{-4}$  (eq. 40), and the  $k = 2$  rms Schottky current for  $10^{11}$  particles and  $\nu_r = 50$  kHz.

$$\langle I_{nk}^2(\omega_{nk}) \rangle = \frac{qQ\omega_r^2}{2} \exp(-\omega_{nk}^2 \sigma_\tau^2) I_k(\omega_{nk}^2 \sigma_\tau^2). \quad (45)$$

Equations 44 and 45 have several interesting features. First, since  $Q = qP$ , the rms current is proportional to  $\sqrt{P}$  as expected from shot noise. In contrast to eq. 38 that depends on unknown constants (e.g.  $A_2$  in eq. 39), the noise calculation is absolute. Equation 44 gives the noise current, and currents above this value are due to phase space structure. This is illustrated in Figure 9 where the current from a quadrupole structure with  $A_2 = 10^{-4}$  is larger than Schottky noise for  $\omega\sigma_\tau < 3.5$ . If  $A_2 = 10^{-5}$  the cross over point would move to  $\omega\sigma_\tau \sim 2.0$ .

## Transverse Phase Space Structure

Analyses of Schottky noise and signals associated with phase space structure can be performed for transverse motion also. The Schottky analysis is an extension of the previous section and is not repeated here. It can be found in Ref. 2. The signals from transverse phase space structure introduce new ideas and are treated in this section.

In general, a 4-dimensional phase space density,  $\kappa$ , must be used to calculate the transverse signal because eq. 32 depends on the betatron amplitude and phase and the synchrotron amplitude and phase



$$\mathbf{D}(\omega) = \omega_r \sum_{n,k=-\infty}^{\infty} \delta(\omega - (n\omega_r + k\omega_s + \omega_\beta)) \int A_\beta dA_\beta d\psi \tau_a d\tau_a d\varphi \quad (46)$$

$$\times \kappa(A_\beta, \psi, \tau_a, \varphi) A_\beta e^{j\psi + jk\varphi} J_k((\omega - \omega_\beta - \omega_\xi)\tau_a) .$$

The phase space density can be expanded in a Fourier series in  $\psi$  and  $\varphi$ . The only component of the  $\psi$  expansion with a non-zero dipole moment is the one with symmetry  $\exp(-j\psi)$ . All of the others equal zero when the  $\psi$  integral in eq. 46 is performed. Each of the components of the  $\varphi$  expansion can produce a signal, and, as in eq. 38, there is a relation between phase space structure and sidebands.

The new aspect is that the betatron amplitude can depend on the synchrotron amplitude,  $A_\beta = A_\beta(\tau_a)$ . In general, coherent transverse modes have such dependencies.<sup>4</sup> As a specific example consider all of the particles oscillating with the same amplitude,  $A_0$ , and a Gaussian distribution in  $\tau_a$  (eq. 35) with no  $\varphi$  dependence. The phase space density is

$$\kappa = \frac{1}{(2\pi)^2} \rho_0(\tau_a) \delta(A_\beta - A_0) e^{-j\psi} , \quad (47)$$

and

$$\mathbf{D}(\omega) = \omega_r A_0 Q \sum_{n=-\infty}^{\infty} \delta(\omega - (n\omega_r + \omega_\beta)) \exp\left(-\frac{(\omega - \omega_\beta - \omega_\xi)^2 \sigma_\tau^2}{2}\right) . \quad (48)$$

The envelope is a Gaussian centered at  $\omega = \omega_\beta + \omega_\xi \approx \omega_\xi$  and shifts as the chromaticity changes.

The transverse displacement at  $t = 0$  is (eqs. 25 and 30)

$$r_\perp(t=0) = A_\beta e^{j\psi_\beta(t=0)} = A_\beta e^{j(\psi + \omega_\xi \tau_a \cos \varphi)} = A_\beta e^{j(\psi + \omega_\xi \tau)} . \quad (49)$$

The connection between the transverse displacement and the shift of envelope with chromaticity can be understood by plotting the dipole moment,  $\rho_0 r_\perp$ , for different chromaticities and at different times. This is done in Figure 10. When  $\xi = 0$ , the transverse motions of all the particles are in phase. The signal has an average value, i.e. a component at  $\omega = 0$ ; the time scale of the dipole moment is the bunch length,  $\sigma_\tau$ , and the characteristic frequency is  $\omega \sim 1/\sigma_\tau$ . As the chromaticity increases a head-to-tail phase shift is introduced, and the head and tail are out of phase. The average value of the signal decreases thereby decreasing the signal at  $\omega = 0$ . In addition, the dipole moment varies more rapidly along the bunch. This shortens the time scale and increases the characteristic frequency; the envelope has shifted to higher frequency as given by eq. 48.

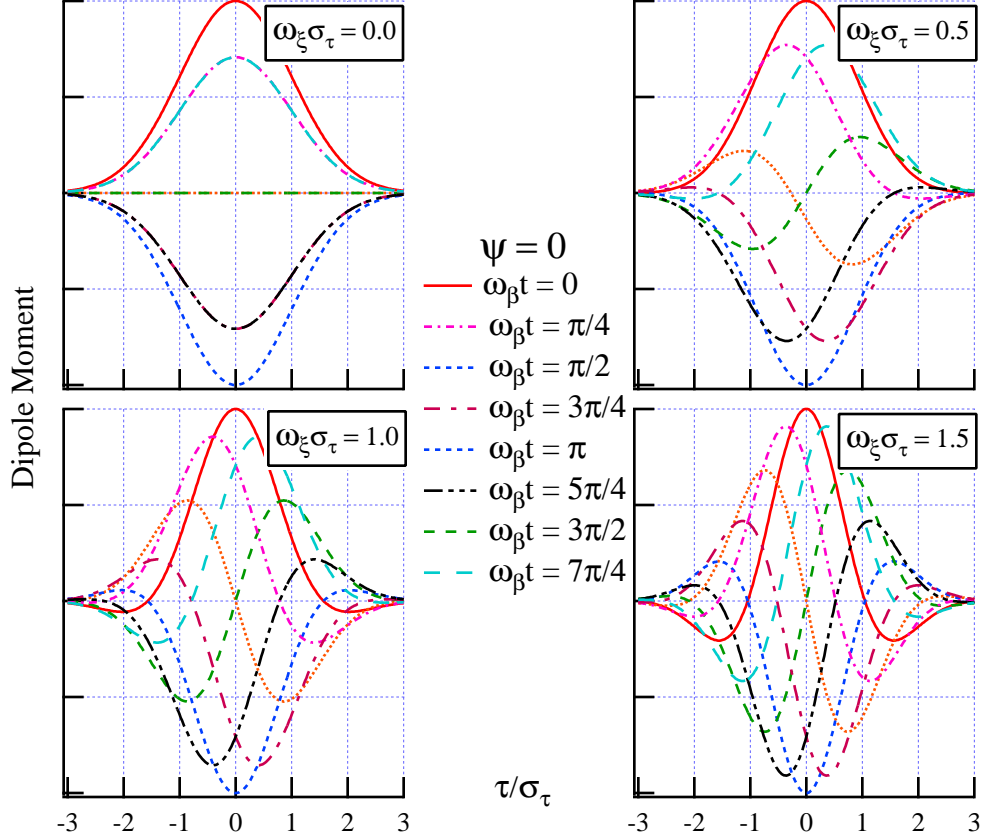


**Figure 10.** The dipole moment at different times for different values of chromaticity.

## Coupled Bunch Signals

The examples above have all involved convolution of single particle signals with the beam phase space density. The final one goes back to the derivation leading to eq. 19. Assume that the beam has 2 equally spaced bunches each of which can be treated as a macroparticle and that these bunches are coupled together by a long range wakefield. The phase shift between bunches,  $\Delta\phi$ , can have only discrete values from the following argument. If the phase of the first bunch is  $\phi$ , the phase of the second bunch is  $\phi + \Delta\phi$ , and the phase of the third bunch is  $\phi + 2\Delta\phi$ . The third bunch is the same as the first bunch, so the possible values for  $\Delta\phi$  are  $\Delta\phi = 0, \pi$ . The first bunch current is given by eq. 19. Assuming the second bunch has the same amplitude, its current is given by eq. 18 with a phase factor  $\exp[j(k\Delta\phi + jn\omega T/2)]$  multiplying it. The first term is the bunch-to-bunch phase shift, and the second is due to the arrival time delay of the second bunch. Adding these two currents together gives

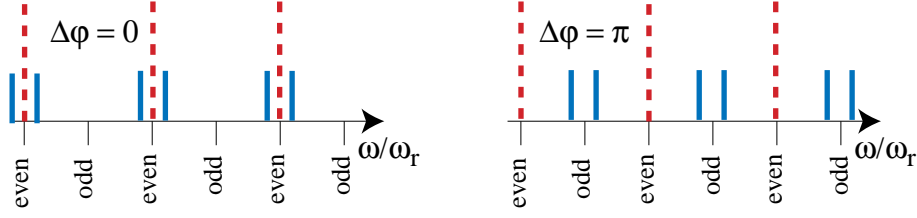


**Figure 11.** The two bunch spectra for coupled bunch modes with 0 and  $\pi$  phase shift between bunches.

$$I_b(\omega) = \omega_r \sum_{k,n=-\infty}^{\infty} e^{jk(\varphi-\pi/2)} J_k(\omega\tau_a) (1 + e^{j(k\Delta\varphi+\omega T/2)}) \delta(\omega - k\omega_s - n\omega_r). \quad (50)$$

For rotation harmonics the phase difference between bunches doesn't matter, the current equals zero when  $n$  is odd, and it is double the single bunch current when  $n$  is even. The latter two follow from  $n\omega_r T/2 = n\pi$ . When  $k = \pm 1$ , the sidebands of the odd rotation harmonics are present if  $\Delta\varphi = \pi$  and are missing (neglecting a factor  $O(\omega_s T/2)$ ) if  $\Delta\varphi = 0$ . The sidebands of the even rotation harmonics are missing if  $\Delta\varphi = \pi$  and present if  $\Delta\varphi = 0$ . This is illustrated in Figure 11. The presence or absence of particular sidebands tells the relative motion of the bunches.

This analysis can be generalized to many bunches. For  $B$  bunches the possible values for the phase shift between bunches are  $\Delta\varphi = 2\pi m/B$  where  $m = 0, \dots, B - 1$  is called the coupled bunch mode number. Only every  $B$ th rotation harmonic appears, and if one sees synchrotron sidebands of the  $n$ th rotation harmonic it is from a coupled bunch mode with mode number  $n = \text{mod}(n, B)$ . This follows because the phasors representing the current of the individual bunches have the same phase and add up coherently only when

$$\Delta\varphi + \frac{n\omega_r T}{B} = \frac{2\pi m}{B} + \frac{2\pi n}{B} = 2\pi p; \quad p = \text{integer}. \quad (51)$$

If bunches are unequally spaced or have different charges or amplitudes, these simple results may not hold, but the same phasor addition can be used to identify dominant lines for different couple bunch modes.

## CONCLUDING REMARK

There is a wealth of information in the beam spectrum. The techniques used in the examples above can be applied and/or extended to chromaticity measurements, coherent frequency shifts, etc. In addition, there is a close relationship between beam generated signals and beam stability because it is the current and dipole moment that drive accelerator impedances and produce forces that act on the beam.

These paper was intended to introduce ideas and methods for understanding beam spectra. I hope it serves that purpose.

## REFERENCES

1. I. S. Gradshteyn and I. M. Ryshik, Tables of Integrals, Series, and Products (New York: Academic Press, 1965), eq. 8.511.4.
2. R. H. Siemann, AIP Conference Proceedings **184** (New York, 1989, edited by M. Month and M. Dienes), p. 430.
3. Reference 1, eq. 6.631.4
4. J. L. Laclare, 11th International Conference of High-Energy Accelerators (Basel: Birkhauser Verlag, 1980, edited by W. S. Newman), p. 526.
5. Reference 1, eq. 6.633.2